International Journal of Modern Research in Engineering and Technology (IJMRET)
www.ijmret.org Volume 10 Issue 08 ǁ August 2025.

Taguchi L9 Optimization Approach on Biodiesel Production from Jatropha Curcas Oil

Polycarp Ikechukwu Nwabuokei[1], Onoriode Erhinyodavwe[2], Richard Eluojo Asenime[3] & Blessed Akhere Omashavire[4]

[1]*Department of Chemical Engineering, Faculty of Engineering, University of Delta, Agbor, Delta State, Nigeria.*
[2]*Department of Mechanical Engineering, Faculty of Engineering, University of Delta, Agbor, Delta State, Nigeria*
[3]*Department of Mechanical Engineering, Faculty of Engineering, University of Delta, Agbor, Delta State, Nigeria*
[4]*Department of Chemical Engineering, Faculty of Engineering, University of Benin , Benin city, Edo State, Nigeria.*

ABSTRACT: This research work studied the production and optimization of biodiesel from Jatropha Curcas oil (JCO) using a heterogeneous bi-functional catalyst synthesized from a blend of snail shells and kaolin. The Jatropha curcas oil was mixed with methanol and catalysts to undergo a tranesterification reaction. The characterization of the Jatropha curcas oil (JCO) was done using American Society Testing Methods (ASTM). The heterogeneous catalyst was also characterized using Scanning Electron Microscope (SEM), the Brunauer-Emmett-Teller (BET), and X-ray diffraction. The transesterification reaction was repeated with varying catalyst weight, oil to methanol ratio, reaction time, and reaction temperature. The optimization of the concurrent esterification and transesterification of Jatropha Curcas oil (JCO) was executed using Taguchi L9 approach, which encompasses the manipulation of four variables, each with three levels, while monitoring two key responses. The biodiesel produced was characterized and compared with biodiesel standards specified by ASTM D6751 and EN 14214. The optimal value of the reaction shows a conversion of 91.32% at a methanol to oil ratio of 12:1. The catalyst used was found to be economically viable after being reuse for 5 run without treatment and still produced a significant yield of 75.39%.

KEYWORDS: Bi-functional catalyst, Taguchi L9 approach, Transesterification reaction, Esterification reaction, Jatropha Curcas oil (JCO).

I. INTRODUCTION

The limited fossil fuel resources along with the need to reduce greenhouse gas emissions were major impulses to the development of alternative fuels. Nowadays, a large amount of biodiesel is produced around the world due to it numerous advantages (Ma and Hanna, 1999; Zhang et al., 2003); and It is also a local renewable source of energy and highly biodegradable (Meng et al., 2008). However, its large scale production has still not been achieved.

Lots of studies and researches have been done on biodiesel production from various catalysts and the outcome has been a subject of concern since there tend to be inconsistencies in the outputs. It can be seen from the outputs that the effects of catalyst types on transeterification process has not been properly looked into. Also a comparative and a process optimization study of the transesterification catalytic processes which is an important goal in improving the quality and reducing production costs in biodiesel production processes needs to be investigated (Mojtaba 2012).

Consequently, since biodiesel can be

produced using various catalyst types, resulting in biodiesel with different properties, it has become necessary to have a standard that will serve as a point of reference for biodiesel that is produced from a defined economically viable catalyst type and operating parameters to guarantee engine performance without difficulty at a moderate cost. Biodiesel produced is not classified as diesel fuel substitute unless they meet the requirements established by standards. Thus the need for comparison of some standard parameters (*Bunkyakiat 2006).*

II. MATERIALS AND METHODS

The Jatropha Curcas oil (JCO) used for this research work was sourced from AgriEnergy in Kano. All chemicals and solvents were purchased from chemical dealers at the chemical and drug market in Onitsha Main Market, Anambra State, Nigeria, and of analytical grade. Additionally, the Snail Shell for the catalyst was sourced locally, and the Clay (Kaolin) obtained from Okija, Anambra State, Nigeria.

A. Determination of Properties and Fatty Acid Composition of Jatropha Curcas Oil and Biodiesel

1. **Determination of Specific Gravity (SG*):*** Specific gravity of the *Jatropha Curcas Oil* and biodiesel was determined using ASTM D4052.

2. ***Determination of Viscosity (μ)****:* The viscosity of the Jatropha Curcas Oil and biodiesel was determined at 40°C using ASTM D445-09. At equilibrium temperature, a digital Vibro viscometer tip was inserted to the sample to measure the dynamic viscosity and the reading was taken from the controller

3. ***Determination of Acid Value (AV)***: The AV of the oil and biodiesel was determined using the method described by IUPAC (1979) and modified by Egan et al.(1981).

4. ***Determination of Saponification Number (SN):***

Indicator method was used as specified by ISO 3657 (1988) to determine the SN of the Jatropha Curcas Oil and biodiesel.

5. ***Determination of Iodine Value (IV):*** The method specified by ISO 3961 (1989) was used to determine the iodine value of the Jatropha Curcas Oil and biodiesel

6. ***Determination of Heating Value (Calorific Value*)*:*** The HHV of the Jatropha Curcas Oil and its biodiesel was determined using the empirical formula suggested by Demirbas (1998), using results of IV and SN

$$HHV = 49.43 - [0.041(SN) + 0.015(IV)] \quad (1)$$

7. The FFA value: The % FFA value was calculated from the acid value" AV" using the following relationship $\%FFA = \frac{AV}{2}$ (2)

B. Chemical Composition of Jatropha Curcas Oil

A standard mixture of these esters was injected into a Shimadzu Gas Chromatograph-Mass Spectrometer (GCMS-QP 2010 Plus). GC for identification and quantification purposes with a flame ionization detector (FID), and the carrier gas helium (30 mL/min.)

C. Catalyst Preparation And Characterization

1. Catalyst Preparation and Impregnation

The kaolin samples obtained from Okija, Anambra State, Nigeria, was dried at ambient temperature for 8 to 10 days, pulverized, sieved, screened to obtain fine particles and activate with formic acid (Gao et al., 2016). Snail Shells (which are majorly composed of Calcium carbonate (Nkansah, Agyei, and Opoku 2021) which are sourced from a local restaurant were used in the synthesis of the basic active site of the bifunctional catalyst.The shells was pulverised manually using a wooden mortar and pestle and the ground shells were calcined at 900 °C for 6 hours. After calcination, they were soaked in 0.5M KOH for 48 hours, the sample underwent filtration and rinsing with distilled water. Afterward, it was subjected to a 150 °C drying process for a duration of 3 hours in an oven. After drying, the sample is taken out of the oven and permitted to cool to the temperature of the surrounding room, and kept in an airtight container.(Akhabue and Ogogo 2018).

The acid and basic precursors produced were mixed in a ratio of 2:1 in a beaker with some addition of water, yielding a wet mixture. The resulting mixture was dried in the oven at 150 0C, then crushed with the wooden mortar and pestle, and then heated up again at 300 0C for 5 hours in the muffle furnace. The sample was then removed and placed in a desiccator to cool, before transferring it to an airtight container.

2. Catalyst Characterization

The Scanning Electron Microscope (SEM) provide insights into the surface properties, chemical composition, crystalline structure, and alignment of the sample's constituents (Swapp et al., 2017); The Brunauer-Emmett-Teller (BET) surface analyser employs nitrogen sorption analysis to provide the precise measurements of surface area of the catalyst; Thermo gravimetric Analysis (TGA) was involved in the continuous monitoring of the catalyst mass; Electron Dispersive Spectroscopy (EDS) helped to analyze the diverse elemental combinations of the catalyst mixture; X-ray diffraction(XRD) was employed to establish the atomic structure in the catalyst crystal; FTIR (Fourier Transform Infrared Spectroscopy) was used to analyze sample interaction with infrared electromagnetic radiation, allowing for the distinction between organic and inorganic compounds present in the catalyst mixture.

D. Biodiesel Production And Optimization

The JCO was gradually heated to a temperature 55ºC within a conical flask, which houses a stir bar placed on a magnetic stirrer, effectively creating a continuously stirred tank reactor (CSTR). Simultaneously, methanol and the prepared bio-based catalyst were then introduced into the reaction mixture.

Under these carefully optimized conditions, the reaction ensues, resulting in the formation of a mixture containing biodiesel, glycerol, and the catalyst. To facilitate the separation of these components, a centrifuge is employed to recover the catalyst, while a separating funnel is employed to isolate the glycerol. The biodiesel is subsequently subjected to a washing process, utilizing warm water, and is then dried, ultimately yielding a purified biodiesel product of high quality. The glycerol by-product is appropriately discarded, while the recovered catalyst is further evaluated for its potential reusability. The optimization of the concurrent esterification and transesterification of JCO was executed using the Taguchi L9 approach, which encompasses the manipulation of four variables, each with three levels, while monitoring two key responses. This method was employed to refine the process and attain the best parameters for producing biodiesel.

Table.1: Taguchi optimization factors and Responses

S/N	Factors	Level 1	Level 2	Level 3	Responses
1	Methanol: Oil Ratio	9:1	12:1	15:1	Yield (%)
2	Catalyst Weight (%)	2%	4%	6%	Acid Value (mg KOH/g)
3	Temperature (^{0}C)	55 ^{0}C	60 ^{0}C	65 ^{0}C	
4	Time (Minutes)	60 Minutes	90 Minutes	120 Minutes	

E. Catalyst Reusability Study.

A larger volume of Jatropha Curcas Oil (JCO) was used, and meticulous calculations were performed to ascertain the necessary quantities of catalyst and methanol. Subsequently, the experiment was conducted, and the catalyst was separated using a centrifuge without undergoing any washing or treatment. It was subsequently reused multiple times and collected for several runs until the biodiesel yield reached a point where it became insignificant. In this study, 'significant' referred to a biodiesel yield of 70% or higher.

III. RESULT AND DISCUSSION

PHYSIOCHEMICAL PROPERTIES OF JATROPHA CURCAS OIL (JCO)

The physical and chemical properties of the Jatropha Curcas Oil (JCO) were analysed as in the previous chapter according to the ASTM standard. Table 2 presents the results obtained from the characterization of the JCO

Table 2: Physiochemical Properties of JCO

PROPERTIES	VALUES
Acid Value (mg KOH/g)	12.15
FFA (%)	6.075
Saponification Value	189.89
Molecular Weight (g)/mol	946.94
Peroxide Value	10
Viscosity at 31ºC (MPa.S)	15.1
Density (Kg/m^3)	904
Moisture Content (%)	7

CATALYST CHARACTERISATION

The physicochemical properties of the catalyst underwent a comprehensive examination. The pore characteristics of the treated catalyst were investigated using the Brunauer-Emmett-Teller (BET) and Barret-Joyner-Halenda (BHJ) techniques, while the temperature-related behavior of the modified catalyst was analyzed with a thermogravimetric analyzer (PerkinElmer TGA4000). Energy Dispersive X-ray Fluorescence (EDXRF) was utilized to analyse the composition of oxides. The crystalline phases in the treated catalyst were identified using X-ray diffraction. Lastly, functional groups incorporated into the treated catalyst were analysed using an FTIR spectrophotometer.

The TGA graph illustrates three distinct phases of weight loss for the treated catalyst. Initially, between 28.59 ºC and 340 ºC, the catalyst loses less than 10% of its weight, primarily due to the removal of absorbed organic molecules and moisture. Subsequently, between 340 ºC and 510 ºC, a significant weight loss occurs, accounting for approximately 80% of the total weight reduction during this period, possibly attributed to additional moisture removal. The third weight loss phase occurs after 510 ºC, coinciding with the catalyst's thermal breakdown phase, with weight loss remaining relatively constant beyond 700 ºC until the catalyst ultimately decomposes at approximately 888.4 ºC. The DTA graph exhibits a minor peak around 200 ºC, corresponding to the 10% weight loss observed in the TGA graph, and a more prominent peak at 410 ºC, indicating an endothermic reaction likely linked to the catalyst's decomposition, consistent with the thermal breakdown observed in the TGA graph.

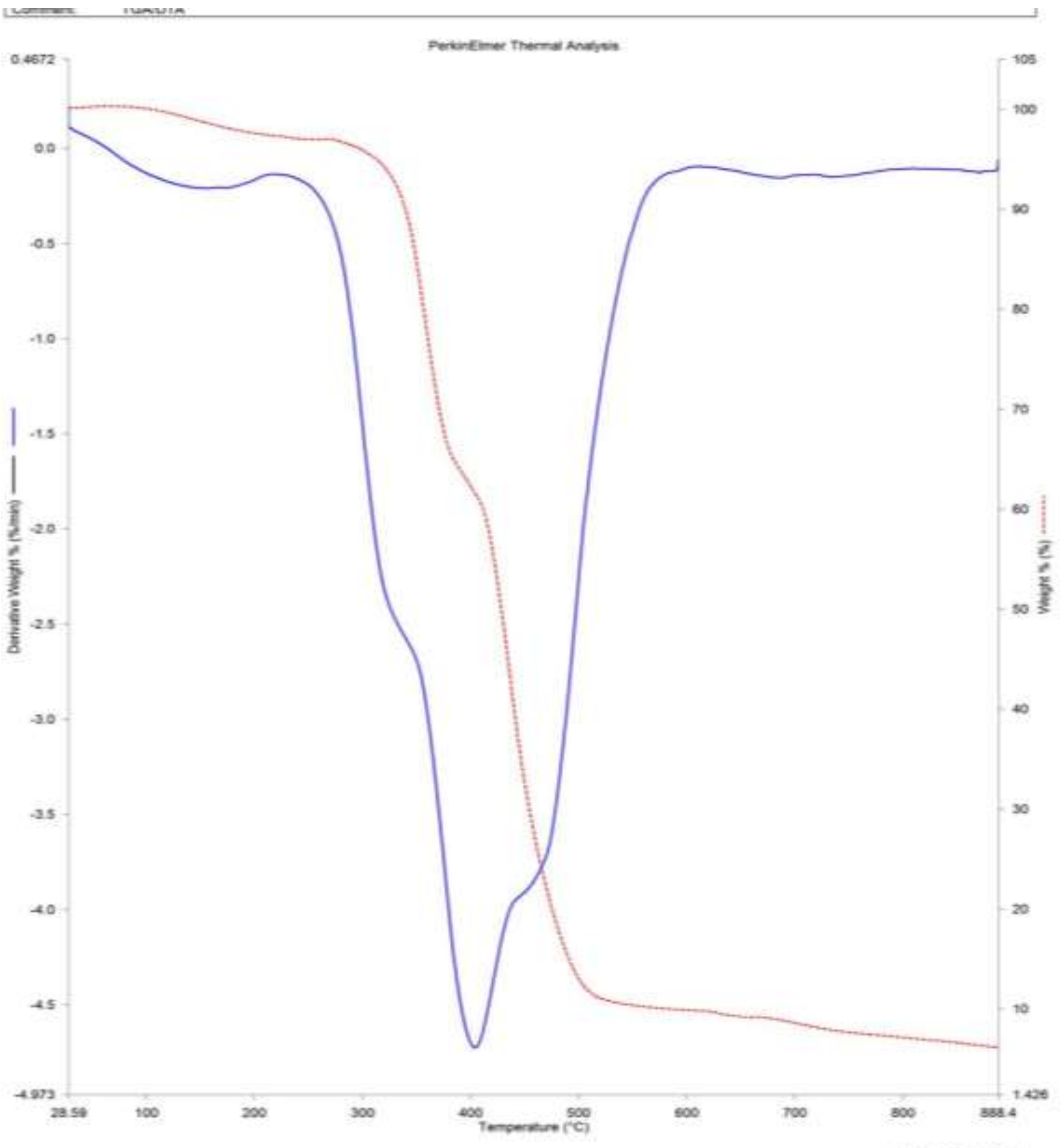

21/09/2023 18:45:33

Figure.1: TGA/DTA plots for the unused catalyst

Table 3: Illustrates the various oxides and their corresponding concentrations in the processed catalyst as determined by the EDXRF analysis. According to the table, the two most abundant basic oxides in the catalyst were potassium oxide (4.008%) and calcium oxide (86.811%). There were also trace amounts of Na_2O, MgO, SiO_2, SnO_2, and SrO present.

Table 3: Results of EDXRF Analysis on the synthesized catalyst

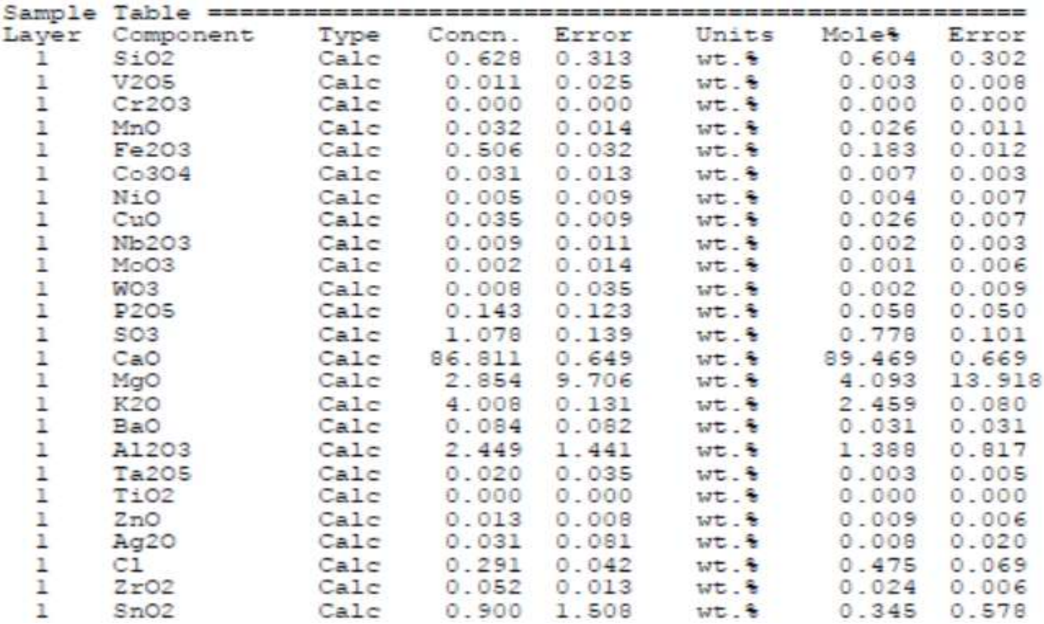

```
Sample Table ==================================================
Layer  Component     Type    Concn.   Error     Units    Mole%   Error
  1    SiO2          Calc     0.628   0.313     wt.%     0.604   0.302
  1    V2O5          Calc     0.011   0.025     wt.%     0.003   0.008
  1    Cr2O3         Calc     0.000   0.000     wt.%     0.000   0.000
  1    MnO           Calc     0.032   0.014     wt.%     0.026   0.011
  1    Fe2O3         Calc     0.506   0.032     wt.%     0.183   0.012
  1    Co3O4         Calc     0.031   0.013     wt.%     0.007   0.003
  1    NiO           Calc     0.005   0.009     wt.%     0.004   0.007
  1    CuO           Calc     0.035   0.009     wt.%     0.026   0.007
  1    Nb2O3         Calc     0.009   0.011     wt.%     0.002   0.003
  1    MoO3          Calc     0.002   0.014     wt.%     0.001   0.006
  1    WO3           Calc     0.008   0.035     wt.%     0.002   0.009
  1    P2O5          Calc     0.143   0.123     wt.%     0.058   0.050
  1    SO3           Calc     1.078   0.139     wt.%     0.778   0.101
  1    CaO           Calc    86.811   0.649     wt.%    89.469   0.669
  1    MgO           Calc     2.854   9.706     wt.%     4.093  13.918
  1    K2O           Calc     4.008   0.131     wt.%     2.459   0.080
  1    BaO           Calc     0.084   0.082     wt.%     0.031   0.031
  1    Al2O3         Calc     2.449   1.441     wt.%     1.388   0.817
  1    Ta2O5         Calc     0.020   0.035     wt.%     0.003   0.005
  1    TiO2          Calc     0.000   0.000     wt.%     0.000   0.000
  1    ZnO           Calc     0.013   0.008     wt.%     0.009   0.006
  1    Ag2O          Calc     0.031   0.081     wt.%     0.008   0.020
  1    Cl            Calc     0.291   0.042     wt.%     0.475   0.069
  1    ZrO2          Calc     0.052   0.013     wt.%     0.024   0.006
  1    SnO2          Calc     0.900   1.508     wt.%     0.345   0.578
```

The processed catalyst exhibited a significant catalytic potential because of its extensive surface area, with a BET surface area of 722.5 square meters per gram. Additionally, it possessed a pore volume of 0.3998 cubic centimeters per gram and a pore diameter measuring 2.126 nanometers. The average micropore size was 6.296 nm in width with a volume of 0.2848 cubic centimeters per gram (cc/g), and the surface area of micropores measured 801.4 m^2/g. as shown in Fig. 3 below

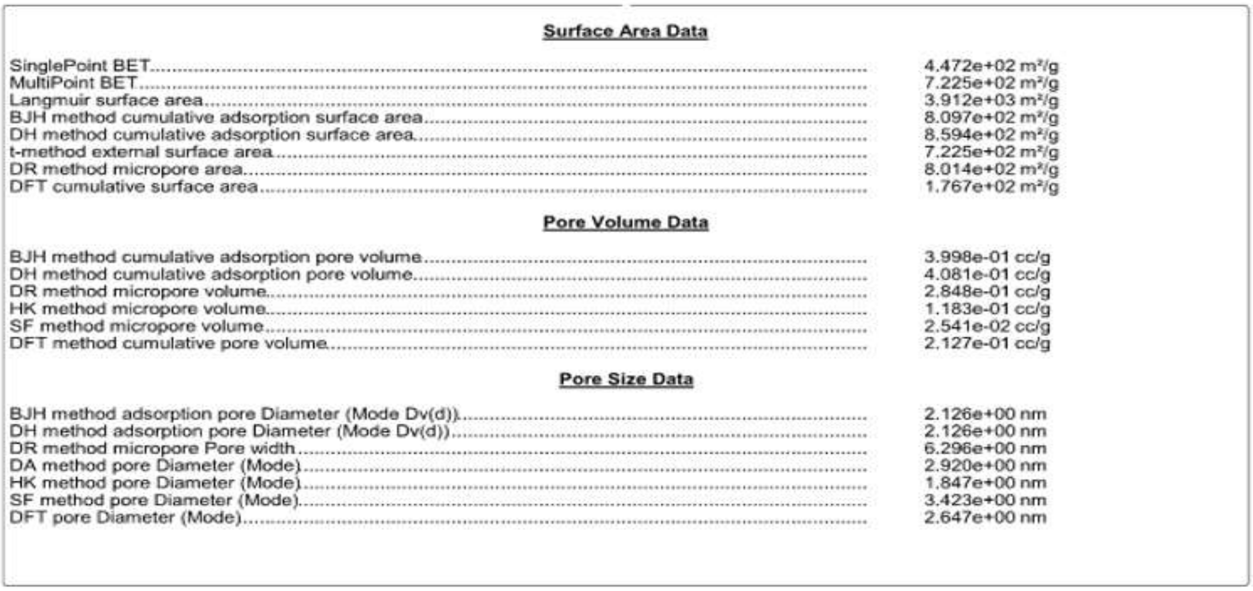

Surface Area Data

SinglePoint BET	4.472e+02 m²/g
MultiPoint BET	7.225e+02 m²/g
Langmuir surface area	3.912e+03 m²/g
BJH method cumulative adsorption surface area	8.097e+02 m²/g
DH method cumulative adsorption surface area	8.594e+02 m²/g
t-method external surface area	7.225e+02 m²/g
DR method micropore area	8.014e+02 m²/g
DFT cumulative surface area	1.767e+02 m²/g

Pore Volume Data

BJH method cumulative adsorption pore volume	3.998e-01 cc/g
DH method cumulative adsorption pore volume	4.081e-01 cc/g
DR method micropore volume	2.848e-01 cc/g
HK method micropore volume	1.183e-01 cc/g
SF method micropore volume	2.541e-02 cc/g
DFT method cumulative pore volume	2.127e-01 cc/g

Pore Size Data

BJH method adsorption pore Diameter (Mode Dv(d))	2.126e+00 nm
DH method adsorption pore Diameter (Mode Dv(d))	2.126e+00 nm
DR method micropore Pore width	6.296e+00 nm
DA method pore Diameter (Mode)	2.920e+00 nm
HK method pore Diameter (Mode)	1.847e+00 nm
SF method pore Diameter (Mode)	3.423e+00 nm
DFT pore Diameter (Mode)	2.647e+00 nm

Figure 2 :BET Analysis results for the synthesized catalysts

Figure 3 depicts the XRD analysis plot conducted on the processed catalyst, revealing its crystalline structure. The plot indicates distinct peaks corresponding to the hexagonal layered crystal structure of Calcite $Ca(CO_3)$ at 2 theta values of 23.298, 29.653, 36.252, 39.667, 43.39, 47.364, 57.619, and 64.85. Additionally, the XRD examination also detects the existence of additional minerals and substances within the catalyst, such as Lime (CaO), Quartz (SiO_2), and Periclase (MgO).

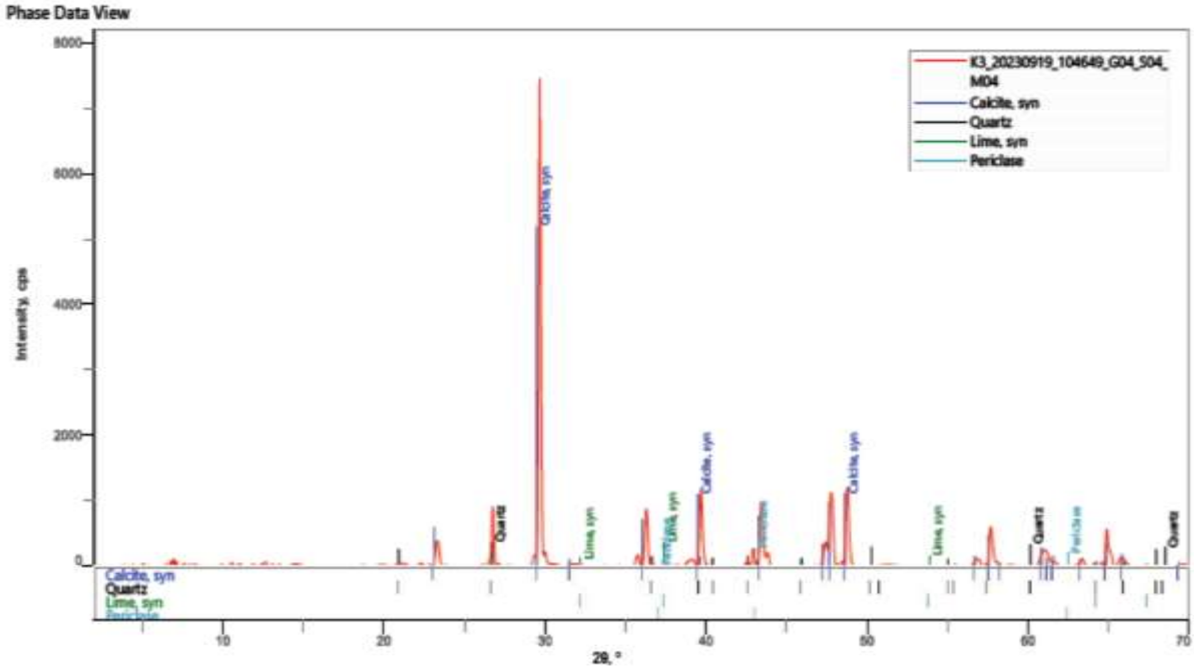

Figure.3: XRD Analysis results for the synthesized catalyst.

MODELING OF SIMULTANEOUS ESTERIFICATION AND TRANS-ESTERIFICATION OF JCO

Robust Design (Taguchi L9 orthogonal array) was used to conduct a statistical analysis of the simultaneous esterification and transesterification of JCO utilising a bifunctional catalyst produced from Snail Shell and kaolin. Employing Design Expert 13.0, an experimental design using Taguchi was carried out. Eq. (3) provides the overall quantity of experiments to be conducted, which varies based on the quantity of levels and factors.

$$F = (G-1)\,H + 1 \qquad (3)$$

Where "F represents the overall count of experiments, G signifies the quantity of levels, and H denotes the quantity of factors". The set values and responses obtained are shown in Table 4. For Jatropha Curcas Oil Biodiesel (JACOB) yield and Acid value as responses

Table 4. Experimental design matrix developed by Taguchi L9 orthogonal array

Run No.	FACTORS				RESPONSES	
	A: MeOH: Oil (mol/mol)	B: Cat. Loading (wt.%)	C: Temperature (ºC)	D: Time (min)	JCOB yield (wt.%)	Acid Value (mg KOH/g)
1	9:1	2	55	60	73.41	0.671
2	15:1	6	60	60	86.41	0.406
3	15:1	2	65	90	86.83	0.543
4	15:1	4	55	120	83.67	0.623
5	9:1	6	65	120	76.94	0.843
6	12:1	2	60	120	86.73	0.697
7	12:1	6	55	90	84.72	0.564
8	12:1	4	65	60	87.63	0.573
9	9:1	4	60	90	80.23	0.726

The collected data were then analysed using analysis of variance (ANOVA) to assess the impact of different elements on the outcomes as presented in Table 5 (a) and Table 5 (b) below.

Table 5(a) results for the analysis of variance (ANOVA) for JCOB yield

Source	Sum of Squares	df	Mean Square	F-value	P-value	
Model	193.35	4	48.34	24.02	0.0047	Significant
A-MeOH: Oil	167.80	2	83.90	41.69	0.0021	
C-Rxn. Temperature	25.55	2	12.77	6.35	0.0574	
Residual	8.05	4	2.01			
Cor Total	201.40	8				

Table 5(b) results for the analysis of variance (ANOVA) for Acid value

Any factor's effect on the response can be described using the sum of squares and the corresponding F-value. Higher F-values and the sum of squares suggest that a component is crucial to the response of the process. Using the probability value, each component's importance to the outcome was also determined (P-value). In statistical analysis, model terms are considered statistically significant if the P-value is below 0.0500. Values above 0.1000 show the non-importance of the model terms. A model may be improved via model reduction if it contains many unnecessary terms.

The ANOVA analysis revealed the sum of squares for JCOB Yield and Acid Value to be 193.35 and 0.1206, accompanied by F-values of 24.02 and 21.90, along with corresponding P-values of 0.0047 and 0.0056, respectively. From the analysis of variance carried out on JCOB yield and Acid Value results, it can be seen that The yield of JCOB was notably influenced by the ratio of methanol to oil and the temperature of the reaction process, where the methanol to oil ratio was found to have the greatest impact on the JCOB yield (which was also verified by (Falowo, 2021) with a sum of squares value of 167.80, F-value of 41.69, and P-value of 0.0021, while the methanol to oil ratio and the reaction time reaction temperature contributed significantly to the acid value, where reaction temperature was found to contributed more with a sum of squares value of 0.0755, F-value of 0.0755 and P-value of 0.0046.

The elevated levels of components are denoted as +1 by default, while their lower levels are represented as -1. This allows for a comparison of factor coefficients and an evaluation of their impact, the relative significance of the components, and the use of the coded equations.

Source	Sum of Squares	df	Mean Square	F-value	p-value	
Model	0.1206	4	0.0301	21.90	0.0056	Significant
A-MeOH: Oil	0.0755	2	0.0378	27.44	0.0046	
D-Rxn. Time	0.0451	2	0.0225	16.37	0.0119	
Residual	0.0055	4	0.0014			
Cor Total	0.1261	8				

JCOB yield (wt.%) = 82.952 - 6.092A[1] + 3.4078A[2] - 2.352 C[1] + 1.504 C[2] (4.a)

AV (mg KOH/g) = 0.6273 + 0.1193 A[1] - 0.016A[2] - 0.0773 D[1] - 0.0163 D[2]] (4.b)

Where A[1] and A[2] are the first and second levels of methanol to oil ratios, respectively; B[1] and B[2] are the first and second levels of catalyst loadings; C[1] and C[2] are the first and second levels of reaction temperatures; and D[1] and D[2] are the first and second levels of reaction time, respectively.

PREDICTED VERSUS ACTUAL VALUES OF JCOB YIELD AND ACID VALUE

In Figure 4, the predicted AVs and JCOB yields are plotted against the actual value as Tabled in Table 6. Figure 4a and Figure 4b illustrate the predicted and actual values for the JCOB yield and the AV of the JCOB, respectively. The majority of the data points in both plots were near the line, demonstrating the high relevance of the models.

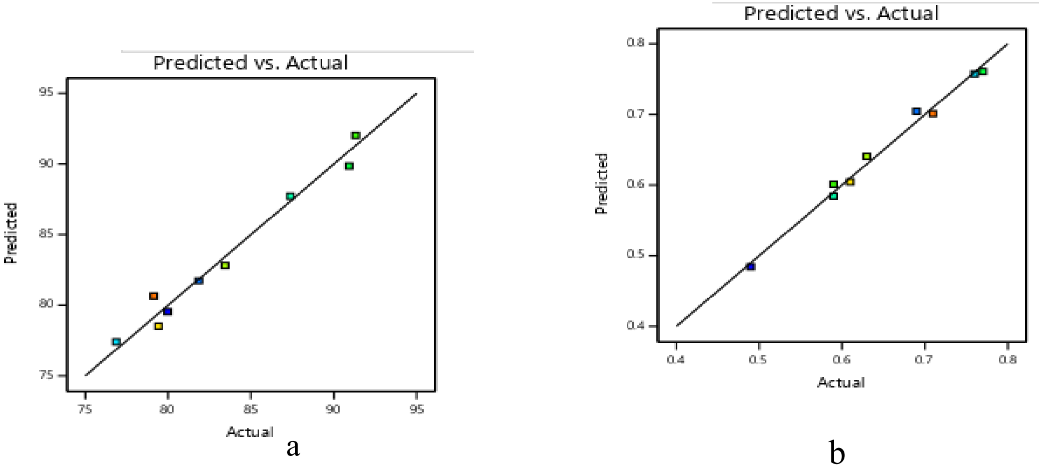

a

b

Figure 4. Values predicted versus actual for (a) JCOB yield (b) AV

Run No.	FACTORS				ACTUAL JCOB yield (wt.%)	PREDICTED JCOB yield (wt.%)
	A: MeOH: Oil (mol/mol)	B: Cat. Loading (wt.%)	C: Temperature (°C)	D: Time (min)		
1	18:1	3	60	60	79.14	80.64
2	6:1	1	55	60	79.98	79.54
3	12:1	1	60	180	87.38	87.73
4	12:1	3	55	120	91.32	92.04
5	18:1	1	65	120	83.44	82.83
6	6:1	3	65	180	76.88	77.42
7	18:1	2	55	180	79.42	78.52
8	12:1	2	65	60	90.92	89.85
9	6:1	2	60	120	81.84	81.73

Table 6a Values for Predicted and Actual JCOB Yields (wt.%)

Run No.	**FACTORS**				**ACTUAL Acid Value (mg KOH/g)**	**PREDICTED Acid Value (mg KOH/g)**
	A: MeOH: Oil (mol/mol)	**B: Cat. Loading (wt.%)**	**C: Temperature (ºC)**	**D: Time (min)**		
1	18:1	3	60	60	0.71	0.7011
2	6:1	1	55	60	0.49	0.4844
3	12:1	1	60	180	0.59	0.5844
4	12:1	3	55	120	0.59	0.6011
5	18:1	1	65	120	0.63	0.6411
6	6:1	3	65	180	0.76	0.7578
7	18:1	2	55	180	0.61	0.6044
8	12:1	2	65	60	0.77	0.7611
9	6:1	2	60	120	0.69	0.7044

Table 6b Values for Predicted and Actual Acid Values (mg KOH/g)

FIT STATISTICS

The results for the fitness of the study are shown in Table 7 showing how well the statistical model predicts the set of observations. It shows that both generated models' correlation coefficients (R^2) were higher than 0.90. Less than 0.2 separated the adjusted R^2 value from the expected R^2 value, indicating that the two numbers were reasonably congruent.

Parameters	Value	
	JCOB yield	AV
R^2	0.9747	0.9893
Adjusted R^2	0.9494	0.9786
Predicted R^2	0.8718	0.9459
Adeq. Precision	16.4022	27.8390
Std. Dev.	1.2	0.0133
Mean	83.37	0.6489
C.V. %	1.43	2.05

Table 7 Fit Statistics of this study

PROCESS PARAMETER OPTIMIZATION AND MODEL VALIDATION

The optimal condition determined using Robust Design (Taguchi L9 orthogonal array) shows: methanol-to-oil molar ratio of 12:1, 1% catalyst loading, A temperature of 55 degrees Celsius and a specific duration for the reaction of 120 minutes, resulting in a JCOB yield of 92.038 wt.% and an AV of 0.484 mg KOH/g. This prediction was validated through a test run of the simultaneous reaction using 50g of JCO under the predicted conditions, yielding a JCOB yield of 93.67 wt.% and an AV of 0.479 mg KOH/g. Additionally, a reusability study with 300g of JCO under the predicted conditions yielded an average JCOB yield of 95.27 wt.% and the acid value is measured at 0.452 milligrams of potassium hydroxide per gram (mg KOH/g).

CHARACTERISATION OF JCOB

Table 8 below shows the results of the physicochemical characterization of JCOB produced using standard testing methods

Table 8: Physiochemical properties of Biodiesel obtained

Acid Value (mg KOH/g)	0.54
FFA (%)	0.27
Saponification Value	114.27
Viscosity at 31^{0}C (MPa.S)	4.42
Density (Kg/m^3)	836
Moisture Content (%)	0.001
Iodine Value	91.28
Pour Point (^{0}C)	-9.4
Cloud Point (^{0}C)	-1.9
Flash Point (^{0}C)	121
Cetane Number	75.527
HHV (Calorific Value)	46.33

REUSABILITY OF THE CATALYST ON JCOB YIELD AND ACID VALUE

A reusability study conducted as shown in Table 9 below shows a useful percentage of JOCB yield indicating the economic viability of the synthesised catalyst when subjected to 5 runs.

Table 4.7 Result for reusability study

RUNS	1	2	3	4	5
JCOB YIELD (Wt. %)	95.27	88.36	87.76	84.80	75.39
ACID VALUE (mg KOH/g)	0.41	0.458	0.527	0.533	0.621
JCO MASS (g)	500	300	250	200	150

IV. CONCLUSION

The Taguchi L9 optimization approach on the production of Biodiesel from Jatropha Curcas Oil (JCO) using a bi-functional catalyst was successfully studied. The physicochemical analysis of the biodesel produced shows a high level of similarity when compared with biodiesel standards specified by ASTM D6751 and EN 14214. Despite having a relatively high acid value of 12.15 milligrams of KOH per gram, Jatropha Curcas Oil (JCO) and bi-functional catalyst (snail shell and Kaolin) are suitable candidates for biodiesel production, judging by the high optimal yield and catalyst reusability.

REFERENCES

[1] Akhabue, C. E., & Ogogo, J. A. (2018b). Modelling and optimization of transesterification of palm kernel oil catalysed by calcium oxide derived from hen eggshell wastes. *Ife Journal of Science*, *20*(1), 127. https://doi.org/10.4314/ijs.v20i1.13

[2] Bunkyakiat, Kunchana; et al. (2006). "Continuous Production of Biodiesel via Transesterification from Vegetable Oils in Supercritical Methanol". Energy and Fuels. American Chemical Society. 20 (2): 812–817.

[3] Demirbas A., (1998). "Energy education: Energy concepts and risks of alternative energy resources in Turkey", Energy Education Science and Technology,Vol.

[4] Egan H, R.S Kirk and R Sawyer (1981). Pearson's Chemical Analysis of food. 8th Edn , Churchill livingstone Edinburgh, UK

[5] Gao, W., Zhao, S., Wu, H., Deligeer, W., & Asuha, S. (2016). Direct acid activation of kaolinite and its effects on the adsorption of methylene blue. Geochemistry and Petrology*. Retrieved from: https://www.sciencedirect.com/science/article/abs/pii/S0169131716301065.

[6] Hanna, M.A. and Ma, F. (1999). Biodiesel production: a review. *Bioresource Technology* 70: 1 – 15.

[7] Meng, X., Chen, G. and Wang, Y. (2008). Biodiesel production from waste cooking oil via alkali catalyst and its engine test. *Fuel Processing Technology* 89: 851–857

[8] Mojtaba Mansourpoor1* and Dr. Ahmad Shariati (2012). Optimization of Biodiesel Production from Sunflower Oil Using Response Surface Methodology

[9] Mineral and proximate composition of the meat and shell of three snail species *Nkansah, Marian Asantewah et al. Heliyon, Volume 7, Issue 10, e08149*

[10] Zhang, Y., Dube, M., McLean, D.D. and Kates, M. (2003). Biodiesel production from waste cooking oil: 2. Economic assessment and sensitivity analysis. *Bioresource Technology* 90(3): 229 – 240